PRZEGLĄD GEOFIZYCZNY
Rocznik LXIII 2018 Zeszyt 4

Wojciech DĘBSKI
Institute of Geophysics, Polish Academy of Sciences

Aleksander CIANCIARA
AGH University of Science and Technology

Eugeniusz KOZIARZ
KGHM Polska Miedź S.A. O/ZG „Rudna”

PASSIVE SEISMIC TOMOGRAPHY AT RUDNA COPPER ORE MINE

Introduction

Understanding the mechanical state of rock masses is critically important for the safe operation of mines, especially deep mines (Gibowicz, Kijko 1994). Accordingly, many different techniques have been proposed, tested, and implemented (Dubiński et al. 2001). In particular, geomechanical and geophysical methods that are based on direct measurements of stress or deformation are the most popular (Dubiński et al. 2001). However, these methods require direct access to a given area to install appropriate sensors, limiting their application to a network of underground openings (tunnels, shafts, chambers, etc.). Moreover, this type of monitoring is “local” in the sense that it provides information only for a small area around installed sensors. Monitoring rocks in larger areas is not possible using these methods. On the other hand, seismic events in mines frequently occur far ahead of the exploitation front (Gibowicz, Kijko 1994) where geomechanical and geophysical methods cannot be used. The situation is even more severe for large devastating rock-bursts, which often nucleate far away from exploitation areas. Beyond the seismological effects, it is of great importance to monitor other large-spatial scale physical processes accompa-

nying mining, for example, subsidence of the land surface. Taken together, the need for monitoring large volumes of rock-mass is clear.

Undertaken attempts of predicting the state of rock masses in mines utilize various geophysical methods (Dubiński et al. 2001). Among them, seismic tomography is the popular approach due to its simplicity and reliability (particularly in comparison to other methods). As a basic formulation (used throughout this paper), seismic tomography provides a spatial distribution for seismic wave velocity and (when repeated) its temporal changes. Thus, it provides information on stress accumulation/reduction for a monitored area. Seismic tomography comes in two flavors, active and passive tomography, that each have advantages and disadvantages. Active tomography relies on generating seismic waves via an artificial source (micro-blasts, hammering, etc.) and recording seismic waves using a portable seismic system. Passive tomography relies on seismic waves generated by induced seismic events recorded by permanent seismic networks operated within mines (see for example, Dębski 2013). More detailed velocity images are produced by utilizing active tomography, but the approach is more expensive. In contrast, passive methods are less accurate but lower cost and can utilize existing mining seismic networks without modification. Passive tomography relies on advanced data processing of continuously recorded seismic data and, for this reason, is a very attractive method for mining applications.

Experimental applications of passive tomography imaging began in the late 1990's in the Rudna copper mine and since 2005 it has been performed routinely as a well-established method (Gibowicz 2009). The practical implementation of the method is based on the software developed at the Institute of Geophysics PAS using data provided by the in-mine seismic network operated at the exploitation level. Most seismometers are run at equivalent depths, which is quite favorable for tomographic purposes because it reduces the task to 2D imaging using only horizontal velocity distributions. Although this simplification results in lost information of possible vertical changes within the rock mass, horizontal spatial resolution is gained with respect to the full 3D image. This 2D approach is also justified from a geo-mechanical point of view that predicts for layered geological structures (this is a case of Rudna mine) the largest possible stress/deformation changes in the direct vicinity of the exploitation strata. This is exactly the area well resolved by 2D tomography.

This paper is devoted to describing our experience performing passive seismic tomography at Rudna copper mine. We begin our discussion by presenting a brief overview of the seismic tomography method and the probabilistic inversion technique we use to solve the tomography task at hand. Next, we present short comments on the data and software applicable to this study. Then, examples of tomography images are presented. We conclude with a discussion of further developments for the tomography method used at Rudna copper mine.

Seismic tomography

Seismic velocity tomography is an inversion technique aimed at imaging the spatial distribution of velocity heterogeneities in global, regional, local or even laboratory scale problems (Nolet 1987; Friedel et al. 1996; Bijwaard et al. 1998; Dębski 2002). It relies on high frequency approximation where seismic energy is assumed to propagate along a thin "tube" between source and receiver, called a ray path (Cerveny 2001). The energy travel time between two points provides information on the average seismic velocity along the ray path. If travel time data are available for a number of ray paths probing different parts of the studied area, it is possible to obtain a spatial map (velocity image) for local heterogeneities in the velocity distribution, also called a tomogram.

The basic tomography forward problem formula relates travel time data (Δt) with the slowness distribution (s) (Aki, Richards 2009):

$$\Delta t = \int s(r)\, dr \tag{1}$$

where $s(r)$ denotes slowness (inverse of velocity $s = 1/v$), Δt is the predicted travel time, and the integral is taken along a given seismic ray path. The ray path itself depends on the slowness distribution; consequently, the relationship between Δt and s in Eq. 1 is highly nonlinear, manifesting itself as a bending of the ray path (Cerveny 2001). This effect is often neglected in the case of local seismic tomography if the slowness distribution does not have a large gradient (Cardarelli, Cerrto 2002). Such a simplification makes the tomography problem easier to solve at the cost of slightly reduced sharpness in the tomogram (Maxwell, Young 1993). Under this assumption, having a set of travel time data $\Delta t = (\Delta t_1, \Delta t_2, ..., \Delta t_N)$ recorded for different source-receiver pairs and the discretized slowness distribution (for example, assuming that the imaged area can be described as a set of homogeneous cells), the linear tomography forward problem turns into a set of linear equations:

$$\Delta t_i = \sum_i G^{ij} s_j \tag{2}$$

where $s = (s_1, s_2, \ldots, s_N)$ is the vector of the discretized slowness field and G^{ij} is a matrix whose elements are lengths of fragments of the i^{th} ray passing through the j^{th} cell. An estimation of the slowness parameters, s, is achieved in various ways, although direct algebraic solution and optimization approaches are most often used (Nolet 1987; Iyer, Hirahara 1993). Bayesian methods, based on sampling of the *a posteriori* probability density, are increasingly more popular (Bosch et al. 2000; Zollo et al. 2002). Below, we provide a brief outline of the Baysian method and note that more detailed descriptions are available in the literature (Mosegaard, Tarantola 2002; Dębski 2004; Tarantola 2005).

Linearization of Eq. 1 and the assumption that all error is Gaussian lead to the inversion technique which actually reduces to matrix calculus bases on Eq. 2. This case is important not only due to the simplicity in the underlying mathematics but also because it is possible to calculate *a posteriori* covariance matrix C^p which is useful as an estimator of inversion errors. However, this simple approach is very sensitive to data uncertainties and choice of an initial model. For these reasons, in practical applications the more complex, but much more robust, probabilistic (Bayesian) approach is preferred.

Probabilistic (Bayesian) inversion

The tomography problem, as outlined above, is the inverse task of inferring a set of unknown parameters (slowness vector, s) from a set of measured data (travel times, Δt). In a classical approach, this problem is solved by finding an optimum value $s = s^{opt}$ for which predicted travel times best fit observations. S^{opt} can be determined by any optimization algorithm or, for the linearized case, by solving a set of linear equations (Eq. 2). Either of these approaches has serious limitations (Dębski 2013) and for practical applications where the reliability of results are important, the probabilistic approach should be used.

Probabilistic inverse theory is built around the notion of pieces of information understood according to common sense. The solution of an inverse problem is regarded as a kind of extraction and joining of available information – an inference process. We can quantify this process using the mathematical theory of probability (Tarantola 1987). The most important operational difference between the probabilistic approach and those previously mentioned is the difference in form of the solution. While the algebraic and optimization techniques provide a single, in a sense optimal estimation of each parameter, the probabilistic solution provides a probability distribution over the model space to quantify the "chance" that a given model is the true one. Thus, it provides a natural framework for comparing different models and for estimating inversion uncertainties. Tarantola (2005) and Dębski (2010) have shown that the *a posteriori* probability density function $p(s)$ is the product of the distribution $f(s)$ describing *a priori* information by the likelihood function $L(s)$, which measures to what extent theoretical predictions fit the observed data:

$$p(s) = \text{const.}\, f(s)\, L(s) \tag{3}$$

where the constant represents a normalization of the probability density function. The likelihood function $L(s)$ reads (Tarantola 2005; Dębski 2010):

$$L(s) = \exp\left(-\left\|\Delta t^{obs} - \Delta t(s)\right\|\right) \tag{4}$$

The symbol ||.|| stands for a norm which is employed to measure the "distance" between observed Δt^{obs} and predicted $\Delta t(s)$ data (Kijko 1994). For purpose of the current presentation, the l_1 norm with constant weightings (error variance) is assumed. Then:

$$||\Delta t^{obs} - \Delta t(s)|| = \sum \sigma^{-1} |\Delta t_i^{obs} - \Delta t_i(s)| \tag{5}$$

where σ describes the corresponding data uncertainties.

We use the l_1, instead of the most popular l_2, because this norm generates a "long-tail" probability distribution that can accommodate the existence of outliers without significantly decreasing accuracy of the obtained solution (Dębski 2013). A more exhaustive analysis of this issue is discussed by Dębski (2010).

Knowledge of the $p(s)$ distribution allows not only to find the most likelihood model s^{ml} for which $p(s)$ reaches a maximum (the equivalent of s^{opt} for the optimization or algebraic solution), but also other characteristics. For example, the average model and the *a posteriori* variance which provides a convenient measure of inversion accuracy. These three basic characteristics of the *a posteriori* distribution $p(s)$ are indeed very important.

In most practical cases $p(s)$ is a complicated, multi-parameter function. This leads to more than just a technical problem at this point, namely how best to inspect the *a posteriori* distribution to extract the required information. The most elementary approach relies on the calculation of point estimators, the most useful being the lowest order central moments (Jeffreyes 1988):
the average model:

$$s^{avr} = \int s p(s)\, ds \tag{6}$$

the covariance matrix:

$$C_{ij}^{p} = \int (s_i - s_i^{avr})\,(s_j - s_j^{avr})\, p(s)\, ds \tag{7}$$

The average model (s^{avr}) provides important information on the best fitting model while also including information about other plausible models from the neighborhood of the "best" model. If sub-optimum models, defined as those for which $p(s) \approx p(s^{ml})$, are similar to s^{ml}, then $s^{avr} \approx s^{ml}$. Thus, a simple comparison of s^{avr} and s^{ml} provides a qualitative evaluation for the reliability of the inversion procedure. The more s^{avr} differs from s^{ml}, the more complex and non-bell-shaped the form of the *a posteriori* $p(s)$ is. This immediately implies, in such a case, that more care must be taken when interpreting inversion results, especially inversion uncertainties. In such situations, using confidence levels instead of the covariance matrix is highly recommended (Jeffreyes 1988).

The diagonal elements of the *a posteriori* covariance matrix C_{ii}^{p} are convenient estimators of inversion uncertainties for each component of s^{avr}, while the non-diagonal elements measure the degree of correlation between pairs of parameters.

The average model (s^{avr}) and the covariance matrix (C^{p}), along with the "best-fitting" s^{ml} point estimators discussed above, provide significantly more information than s^{ml}, however, their evaluation requires full knowledge of $p(s)$ in order to calculate the appropriate integrals. At this point, the Monte Carlo sampling technique becomes very useful.

If a more comprehensive description of $p(s)$ is required, the marginal distributions should be calculated because the *a posteriori* marginal distributions provide deeper insights into the form of $p(s)$ than the point estimators. The inspection of marginal distributions is extremely important for the correct interpretation of the tomographic results. The one-dimensional (1D) marginal *a posteriori* distribution is defined by integrating out all but one parameter from $p(s)$:

$$p_i(s_i) = \int p(s) \prod_{j \neq i} ds_j \tag{8}$$

Multi-dimensional marginals are defined in a similar way. It is important to realize that marginal distributions contain the exact same information on s_j as $p(s)$, without the correlation between other parameters (Jeffreyes 1988; Rudziński, Dębski 2011). However, inspections of the full *a posteriori* $p(s)$ and marginal $p_i(s_i)$ are not equivalent (Dębski 2010).

Seismic network and data

The starting point for any tomography imaging is the recorded data. Depending on the considered problem, data can include the full seismic records (full waveform tomography), seismic wave arrival times (velocity tomography), amplitudes of recorded waves or selected spectral characteristics (attenuation tomography), or first pick arrival times (enhanced velocity tomography). In routine applications, however, the most robust and readily available data are preferred. For this reason, mining tomography is most often based on first arrival time data, although an attempt to use different types of data (for example, first pick arrival times) has also been undertaken (Dębski 2002). Such a choice of data leads to the classical velocity seismic tomography, which is capable of reproducing the *P*-wave velocity spatial distribution. For Rudna mine, data for tomography imaging are collected by an underground, digital seismic network composed of 64 vertical sensors located at depths from 550 m to 1150 m, installed at Rudna and Polkowice-Sieroszowice mines. Network sensors include Willmore seismometers MK-II and MK-III. Seismic signals are transmit-

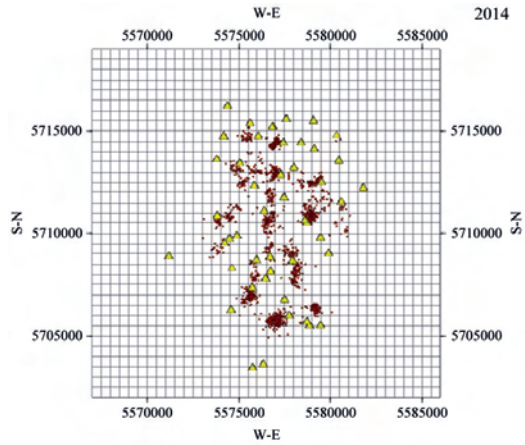

Fig. 1. Underground seismic network (triangles) run by Rudna and Polkowice-Sieroszowice mine in 2014 together with location of seismic events (stars) used for annual passive imaging that year

ted to a central site at the surface where they are digitized by a 14-bit converter across a frequency band of 0.5 to 150 Hz with final dynamics of about 70 dB. The sampling frequency, which determines the absolute accuracy of travel time onset reading, is F = 500 Hz (σ = 2 ms). The uncertainty of event location is better than 100 m, typically around 20 m, and depends on the region. By running most stations at the exploitation level, after disregarding two stations located in the ventilation shaft, we can consider the tomography problem as a two-dimensional one which simplifies data processing and enhances the stability of our obtained velocity images. The seismometer location changes over time following the mining development. For example, the location of seismometers in the first months of 2014 is shown in Figure 1 along with epicenters of events we use for an example of tomography imaging in a scale of the whole mine.

The absolute arrival times picked at a given station (channel) are used together with hypocenter location results to calculate travel time data, the input for our tomography procedure. This standard, widely used approach, introduces some errors to travel time data due to the finite accuracy of the hypocenter locations. To avoid this, and to fully exploit the triggered mode of running the network, we recently began development of a tomography method based on the differences in arrival times. We discuss this issue later on.

Tomography software

Seismic tomography imaging at the Rudna copper main is routinely performed using the MCTOM7 software developed at the IGF PAS. This software

is the computational core responsible for passive tomographic data processing within the computer system maintained by the rockburst prevention unit at the Rudna copper mine. The whole software suite allows, among other things, the detection, location, energy calculation, tomography imaging, and spectral parameter estimation of seismic events occurring within the rock mass in the mine.

The distinguished feature of the MCTOM7 software is the ability to fully utilize the probabilistic approach that allows not only for the construction of a velocity distribution image, but also for a reliable evaluation of the tomographic image quality.

The software operator for the MCTOM program sets control parameters within an appropriate module for the system suite and selects data used for imaging read-out from the system database. MCTOM output provides, among other things, the spatial velocity distribution, imaging errors, and ray paths that are all passed to a graphical module for convenient visualization. The MCTOM software is highly automatic and the role of operator is reduced in most cases to selection of appropriate data and interpretation of the obtained results.

Although MCTOM7 is state-of-the-art for tomographic software in mining applications, there is still room for future improvements. Two essential points are currently under development. The first one is related to an improvement of the quality of imaging results. This point is connected to the fact that one of an important source of imaging errors is the events mis-location. Events mis-location influences the events origin times and thus the observational travel time data Δt^{obs}, introducing observational errors that are difficult to control. As a consequence, the final velocity image can be systematically disturbed. Reducing these types of errors is possible if absolute travel times (as in Eq. 4) are substituted by their differences as initial inputs:

$$\tau_{ij} = T_i - T_j \tag{9}$$

where T_i and T_j are the recorded wave arrival times at i^{th} and j^{th} channel. Although the imaging method based on such differential times is often referred to as "differential tomography", we prefer to call it relative tomography. The advantage of this approach is that event origin time, which appears in T_i and T_j, cancels out and is removed from "relative" data (τ_{ij}). As a result, event origin time does not disturb tomography results. A disadvantage of this approach, however, is that the average signal to noise ratio is smaller for τ_{ij} than for the absolute propagation times, T. However, the method seems to be particularly useful for the Rudna mine application due to the triggering method of seismic event detection implemented in the mining software suite. Work on this issue is currently ongoing.

A second important aspect of tomographic software development deals with the scarcity of data used for tomographic imaging. Clustering of seismic events around exploitation regions, and moderate seismic activity makes it impossible to obtain sharp images of velocity over a relatively short period of time (weeks, months) for small areas of the mine due to insufficient data. We are currently testing the possibility of overcoming this limitation by implementing the so-called box-tomography algorithm (Masson, Romanowicz 2017) in a new version of the software. The idea is to use all available data from the whole mine, but perform imaging only for a small "box" area of interest. In the classical tomography, it is impossible because the imaged area must be large enough to include all seismic sources and stations. Implementation of the box-tomography approach should significantly improve the velocity imaging resolution. Work on this issue is currently very active.

Selected results

To illustrate the tomography technique we describe here, below we present a few examples of tomography imaging at the Rudna mine.

First, let us consider the tomography based on data collected during first 3 months of 2005. Here, we carefully select data for tomography to ensure acceptable data uncertainties using the classical approach based on the absolute travel times. Only events recorded by at least 4 stations are selected to calculate *P*-wave travel time data. The considered events are located using the homogeneous velocity model assuming the *P*-wave velocity of 5800 m/s and location accuracy is about 50 m. Thus, estimation uncertainty for events origin time is about 10 ms. Given this data selection, there are almost 700 ray traces. The constant velocity model with the above-mentioned value is used as the *a priori* model with an assumed uncertainty of 200 m/s. The results in terms of the maximum likelihood and average models are shown in Figure 2. The imaging errors are shown in Figure 3.

This example, corresponding to typical tomographic results, leads to a few important conclusions. The first is that limited data restricts the spatial resolution of classical tomographic imaging in Rudna mine. Second, the obtained images are quite "flat" and strongly biased towards the *a priori* model due to limited data. Finally, this example shows the importance of error estimation for reliably interpreting the obtained tomograms. As shown in Figure 3, the obtained tomograms provide significant information about the velocity distribution only for only a small part of the imaged area where final errors are smaller than the *a priori* ones. This unsatisfactory situation is improved when a differential approach is used, as illustrated by our next example using a newly developed approach.

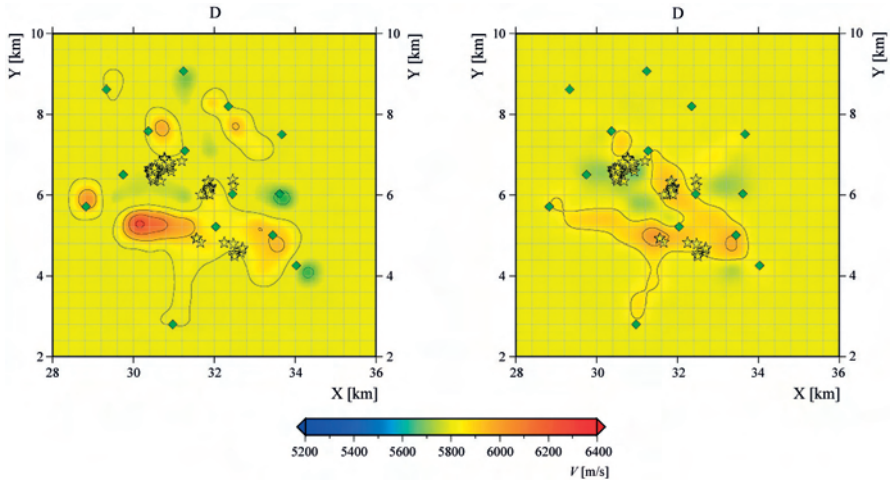

Fig. 2. The maximum likelihood (left) and the average velocity distribution (right) obtained for first 3 months of 2005; relatively small velocity contrast is due to a necessity of strong dumping of the inversion procedure caused by a small number of available ray paths (data)

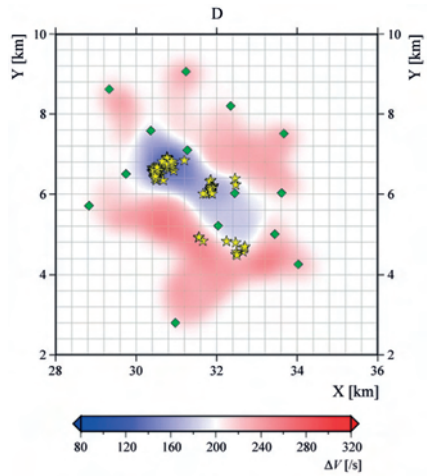

Fig. 3. The spatial distribution of imaging errors; the velocity distribution is well resolved only in the areas where tomography has reduced imaging errors below the *a priori* ones (200 m/s)

In this second example let us consider the tomography performed in 2014 and 2015 based on annually collected data. In this case, we use an experimentally implemented differential mode of a next generation tomography software that allows us to perform tomography imaging using relative travel time data according to Eq. 9. For the tomography of 2014 we use 16490 ray paths

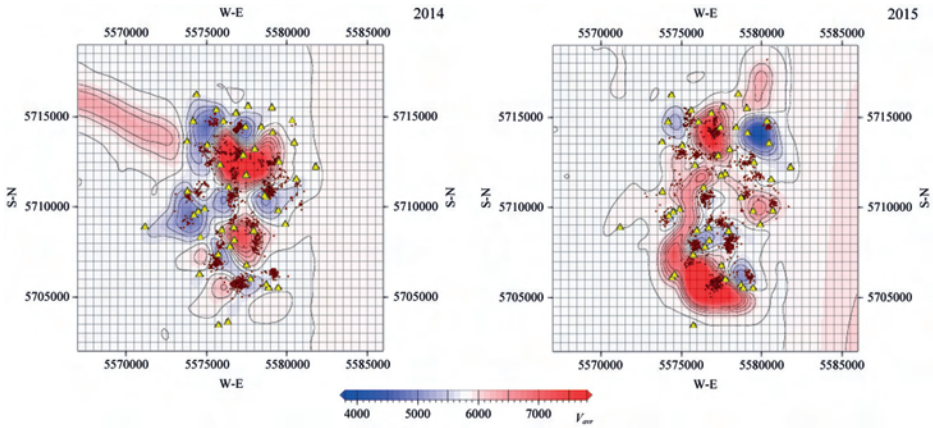

Fig. 4. The average velocity distribution in 2014 (left) and 2015 (right) obtained using annually collected data; comparing of both images clearly indicates migration of a high velocity zone from the central part towards southern part of the mine

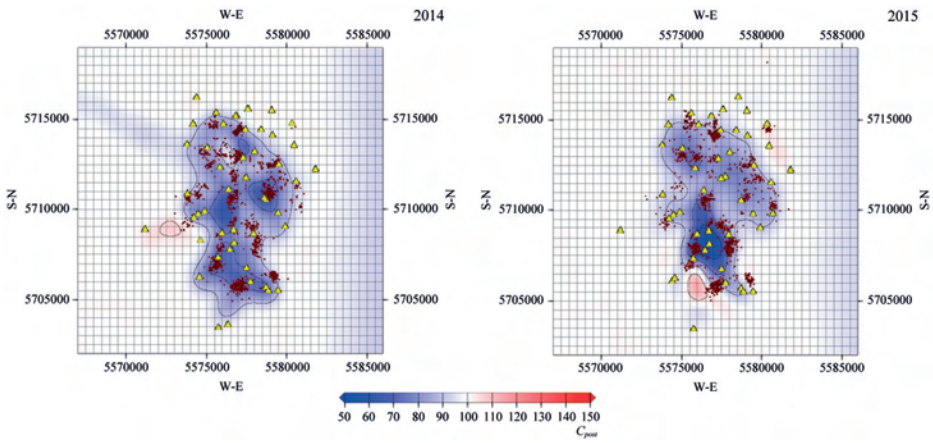

Fig. 5. Tomography imaging errors obtained using annually collected data; in the areas where imaging errors are smaller than the a priori ones, velocity is well resolved by tomography; let us observe that imaging errors are significantly smaller than in case of the traditional tomography based on the absolute travel time data shown in Figure 4

and for 2015, 15752 ray paths. The data include all events with energy $E > 10^3$J. Using such small events is possible because differential travel time data are free of location-induced errors. The obtained average velocity distributions are shown in Figure 4. The corresponding imaging errors are shown in Figure 5.

The use of the differential data allowed us to include the information provided by much smaller events into tomography imaging without a risk of introduction of large errors, as is the case with the classical approach. Consequently, image

quality is significantly improved leading to sharper images and smaller imaging errors with respect to the classical approach.

An interesting effect visible in Figure 4 is an overall migration of a higher velocity zone from the central towards southern part of the mine, while at the same time exploitation developed towards the north in the opposite direction. We currently cannot explain this fact, although many hypotheses can be put forward. Putting aside a broad scale tectonic process change, which cannot be ruled out but is beyond our control, the most probable scenario seems to be a mechanism where velocity increases in the exploited part of the main by a slow deformation (thus stressing) of strata above the mining level. However detailed discussion of this point is beyond the scope of this paper, we mention it here only for demonstration of the method.

Summary

In this paper we briefly describe the effort of performing passive seismic tomography at the Rudna copper mine over the last 10 years. The routine imaging performed at the mine on a weekly, monthly and annual base is not only a tool for helping mining authority to safely run the mine but also provides important scientific information that is useful for advancing seismological analysis.

Continuous development in computational resources and data processing methods results in more efficient and more accurate tomographic results. The recent progress in the development of tomographic imaging based on relative travel times and the box-tomography approach is especially promising We expect that the new generation tomography software, including these advancements, will soon become operationally available and will significantly improve tomographic imaging quality.

Acknowledgments

This paper was partially support by grant No. 2015/17/B/ST10/01946 from the National Science Center, Poland

Literature

Aki K., Richards P.G., 2009, Quantitative seismology, University Science Books, 700 pp.

Bijwaard H., Spakman W., Engdahl E., 1998, Closing the gap between regional and global travel time tomography, Journal of Geophysical Research, 103 (B12), 30055-30078, DOI: 10.1029/98JB02467

Bosch M., Barnes C., Mosegaard K., 2000, Multi-Step samplers for improving efficiency in probabilistic geophysical, [in:] Methods and applications of inversion, P.C. Hansen, B.H. Jacobsen, K. Mosegaard (eds.), Lecture Notes in Earth Sciences, 92, Springer, 50-67

Cardarelli E., Cerrto A., 2002, Ray tracing in elliptical anisotropic media using the linear traveltime interpolation (LTI) method applied to traveltime seismic tomography, Geophysical Prospecting, 50 (1), 55-72, DOI: 10.1046/j.1365-2478.2002.00297.x

Cerveny V., 2001, Seismic ray theory, Cambridge University Press, New York, 722 pp.

Dębski W., 2002, Imaging rock structure using acoustic waves: methods and algorithms, [in:] Seismogenic process monitoring, H. Ogasawara, T. Yanagidani, M. Ando (eds.), CRC Press, 309-326

Dębski W., 2004, Application of Monte Carlo techniques for solving selected seismological inverse problems, Publications of the Institute of Geophysics, Polish Academy of Science, B-34 (367), 207 pp.

Dębski W., 2010, Probabilistic inverse theory, Advances in Geophysics, 52, 1-102, DOI: 10.1016/S0065-2687(10)52001-6

Dębski W., 2013, Bayesian approach to tomographic imaging of rock-mass velocity heterogeneities, Acta Geophysica, 61 (6), 1395-1436, DOI: 10.2478/s11600-013-0148-7

Dubiński J., Pilecki Z., Zuberek W.M. (eds.), 2001, Badania geofizyczne w Kopalniach, IGSMiE PAN, Kraków, 526 pp.

Friedel M., Jackson M.J., Wiliams E.M., Olson M.S., Westman E., 1996, Tomographic imaging of coal pillar conditions: observations and implications, International Journal of Rock Mechanics and Mining Sciences & Geomechanics Abstracts, 33 (3), 279-290, DOI: 10.1016/0148-9062(95)00061-5

Gibowicz S.J., 2009, Seismicity induced by mining: recent research, Advances in Geophysics, 51, 1-563, DOI: 10.1016/S0065-2687(09)05106-1

Gibowicz S.J., Kijko A., 1994, An introduction to mining seismology, Academic Press, 399 pp.

Iyer H.M., Hirahara K., 1993, Seismic tomography: theory and practice, Springer, 864 pp.

Jeffreys H.,1988, Theory of probability, Oxford University Press, 470 pp.

Kijko A., 1994, Seismological outliers: L1 or adaptive Lp norm application, Bulletin of Seismological Society of America, 84 (2), 473-477

Masson Y., Romanowicz B., 2017, Box tomography: localized imaging of remote targets buried in an unknown medium, a step forward for understanding key structures in the deep Earth, Geophysical Journal International, 211 (1), 141-163, DOI: 10.1093/gji/ggx141

Maxwell S.C., Young R.P., 1993, Comparison between controlled source and passive source seismic velocity images, Bulletin of the Seismological Society of America, 83 (6), 1813-1834

Mosegaard K., Tarantola A., 2002, Probabilistic approach to inverse problems, [in:] International handbook of earthquake & engineering seismology. Part A, W. Lee, P. Jennings, C. Kisslinger, H. Kanamori (eds.), Academic Press, 237-265

Nolet G. (ed.), 1987, Seismic tomography with applications in global seismology and exploration geophysics, Springer, Dodrecht, 386 pp.

Rudziński L., Dębski W., 2011, Extending the double difference location technique for mining applications – part I: numerical study, Acta Geophysica, 59 (4), 785-814, DOI: 10.2478/s11600-011-0021-5

Rudziński Ł., Mirek J., Lizurek G., 2017, Identification of seismic doublets occurred on Rudna mine, Poland, Acta Geophysica, 65 (2), 287-298, DOI: 10.1007/s11600-017-0034-9

Tarantola A., 1987, Inverse problem theory: methods for data fitting and model parameter estimation, Elsevier, 613 pp.

Tarantola A., 2005, Inverse problem theory and methods for model parameter estimation, Society for Industrial and Applied Mathematics, Philadelphia, 342 pp.

Wiejacz P., Dębski W., 2001, New observation of Gulf of Gdansk seismic events, Physics of the Earth and Planetary Interiors, 123 (2-4), 233-245, DOI: 10.1016/S0031-9201(00)00212-0

Zollo A., D'Auria L., Matteis R.D., Herrero A., Virieux J., Gasparini P., 2002, Bayesian estimation of 2-D P-velocity models from active seismic arrival time data: imaging of the shallow structure of Mt Vesuvius (southern Italy), Geophysical Journal International, 151 (2), 566-582, DOI: 10.1046/j.1365-246X.2002.01795.x

S u m m a r y

Seismic tomography is a technique widely used to image the Earth's interior at various scales, from the very local subsurface to the whole Earth's interior. Successful tomographic applications in seismology have opened the question of whether, or not, the method can also be helpful in assessing the safety of mining operations. Long-time efforts and accumulated evidence with tomography imaging carried out at the Rudna copper mine clearly indicate that this is really the case. Repeating imaging of velocity distributions reveals that the observed temporal changes provide information that is useful for improving the safety of mining processes. In this paper, we describe our experience of performing seismic passive velocity tomography at the Rudna copper ore mine in the south-western part of Poland. We consider only the last 10 years, when the geophysical unit of Rudna copper mine began using an advanced modern tomography software developed originally for this mine.

Keywords: inverse methods, induced seismicity, seismic tomography.